

SACLANTCEN Report SR - 87

**SACLANT ASW  
RESEARCH CENTRE  
REPORT**



**UNDERWATER PHOTOGRAPHY  
FOR QUANTITATIVE DESCRIPTION  
OF BOTTOM ROUGHNESS**

by  
Tuncay AKAL

1 APRIL 1985

**NORTH  
ATLANTIC  
TREATY  
ORGANIZATION**

**SACLANTCEN  
LA SPEZIA, ITALY**

This document is unclassified. The information it contains is published subject to the conditions of the legend printed on the inside cover. Short quotations from it may be made in other publications if credit is given to the author(s). Except for working copies for research purposes or for use in official NATO publications, reproduction requires the authorization of the Director of SACLANTCEN.

This document is released to a NATO Government at the direction of the SACLANTCEN subject to the following conditions:

1. The recipient NATO Government agrees to use its best endeavours to ensure that the information herein disclosed, whether or not it bears a security classification, is not dealt with in any manner (a) contrary to the intent of the provisions of the Charter of the Centre, or (b) prejudicial to the rights of the owner thereof to obtain patent, copyright, or other like statutory protection therefor.

2. If the technical information was originally released to the Centre by a NATO Government subject to restrictions clearly marked on this document the recipient NATO Government agrees to use its best endeavours to abide by the terms of the restrictions so imposed by the releasing Government.

**Published by**



SACLANTCEN REPORT SR-87

NORTH ATLANTIC TREATY ORGANIZATION

SACLANT ASW Research Centre  
Viale San Bartolomeo 400,  
I-19026 San Bartolomeo (SP), Italy.

tel: national 0187 540111  
international + 39 187 540111  
telex: 271148 SACENT I

UNDERWATER PHOTOGRAPHY  
FOR QUANTITATIVE DESCRIPTION  
OF BOTTOM ROUGHNESS

by  
Tuncay Akal

*(Reprinted from SMITH, P.F. ed. Underwater Photography - Scientific and Engineering Applications. Based on papers presented at a symposium held at the Woods Hole Oceanographic Institution, April 21-24, 1980. New York, NY, Van Nostrand Reinhold Company, 1984: 215-229)*

1 April 1985

This report has been prepared as part of Project 05.



RALPH R. GOODMAN  
Director

TABLE OF CONTENTS

	<u>Page</u>
INTRODUCTION	1
PHOTOGRAPHIC EQUIPMENT AND TECHNIQUES	2
METHOD OF COMPUTATION	2
DISCUSSION OF RESULTS	6
CONCLUSIONS	13
ACKNOWLEDGMENTS	13
REFERENCES	13
APPENDIX - TWO-DIMENSIONAL POWER SPECTRAL DENSITY AND AUTO CORRELATION FUNCTIONS	14

List of Figures

1. General view of the photographic equipment and the frame.	3
2. The method of computation.	4
3. Preprocessing procedures.	5
4. A cosinusoidal test surface, its two-dimensional power spectrum, and autocorrelation function.	7
5. A surface obtained from bottom stereophotographs.	8
6. Another surface from bottom stereophotographs obtained 12 m away from the one shown in Fig. 5, and the results obtained after processing.	9
7. Seafloor with sand waves and the results obtained after processing.	10
8. Another surface from the same area and the results obtained after processing.	11
9. A plaice buried in the sediments, together with its power spectrum and autocorrelation function.	12

# Underwater Photography for Quantitative Description of Bottom Roughness

T. Akal

*SACLANT ASW Research Center  
North Atlantic Treaty Organization  
La Spezia, Italy*

## INTRODUCTION

Knowledge of the roughness of the sea floor is obviously of great importance in marine geology for understanding the processes of the ocean bottom, and in underwater acoustics for understanding the scattering process. The ocean bottom contains a wide spectrum of roughness, ranging from a few millimeters to several kilometers, where small features are superimposed on much larger topographic features (Akal 1984). This complex structure, formed by different physical, chemical, and biological forces, can be quantitatively described in terms of their statistical properties, i.e., power spectral density and autocorrelation functions.

The gross-scale roughness of the sea floor is reasonably well known due to well-developed echo-sounding techniques. However, little is known about small-scale roughness (amplitudes and wavelengths ranging from centimeters to meters) due to the difficulties of measuring them.

The major technique for studying this small-scale roughness is bottom photography. By using photogrammetric techniques, a single pair of overlapping photographs taken with stereo cameras can subsequently be used to provide fine-scale contour charts of the sea floor.

To analyze these contoured charts quantitatively, a numerical method has been developed to calculate the two-dimensional bottom-roughness power-

spectral density and autocorrelation functions (Akal and Hovem 1978). This information gives, quantitatively, two basic parameters of a rough surface: its amplitude and wavelength content and its orientation. These parameters are closely related to the type of sediment and to bottom currents and their direction, hence to the sedimentation, transportation, and erosion processes. This information is also the main parameter for modeling the acoustic bottom scattering and acoustic propagation process.

## PHOTOGRAPHIC EQUIPMENT AND TECHNIQUES

The photographic equipment consists of two EG&G deep-sea cameras, two strobe lights (250 watts each), two battery packs, and a pinger system.

To simplify the photogrammetric analyses, the two cameras are oriented vertically with a fixed base. The strobes are usually placed with a  $25^\circ$  light angle to the field of view, providing the best position for uniform illumination and reducing back-scattering. The whole system is mounted on a sled-type protective frame with two fins to maintain a stable orientation. (Figure 1).

Kodak Ektacolor Professional (type S), and later Vericolor II (5025, type S), negative color films have usually been used. This universal film, which has a speed of 100 ASA (21 DIN), allows high-resolution color prints, black-and-white prints, and color transparencies to be made from one negative.

For maximum resolution the system is usually lowered to a distance of 2 to 4 m above the bottom (using a pinger to control the height) and then allowed to drift over the seafloor.

This system has been operational over the last ten years in different oceans from water depths of a few meters to several thousand meters and has provided high-quality photographs from which the analysis technique has been developed.

## METHOD OF COMPUTATION

Two-dimensional Fourier transforms and correlation functions are straightforward extensions of the corresponding one-dimensional functions. The block diagram in Figure 2 illustrates the methods of computation, which is made in steps: first the  $x$  dependencies are transformed for each  $y$ , and then the  $y$  dependency is transformed. The method of computation is summarized in the Appendix.

Before the computational scheme can begin, the following preprocessing procedures are necessary (Figure 3):

1. Digitization of data. The shapes of the seafloor surface are described by contoured charts. Therefore, an important problem is a simple

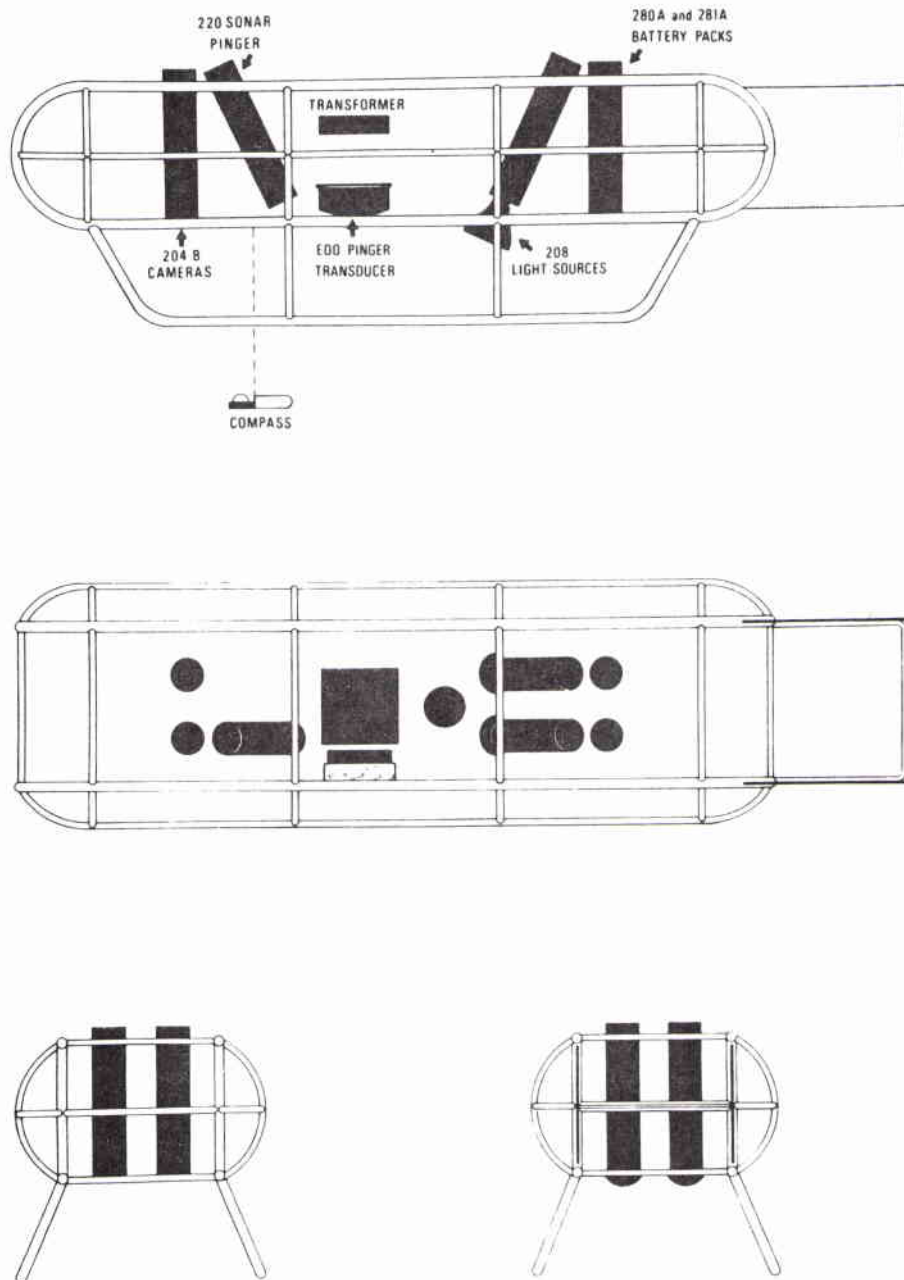


**Figure 1.** General view of the photographic equipment and the frame.

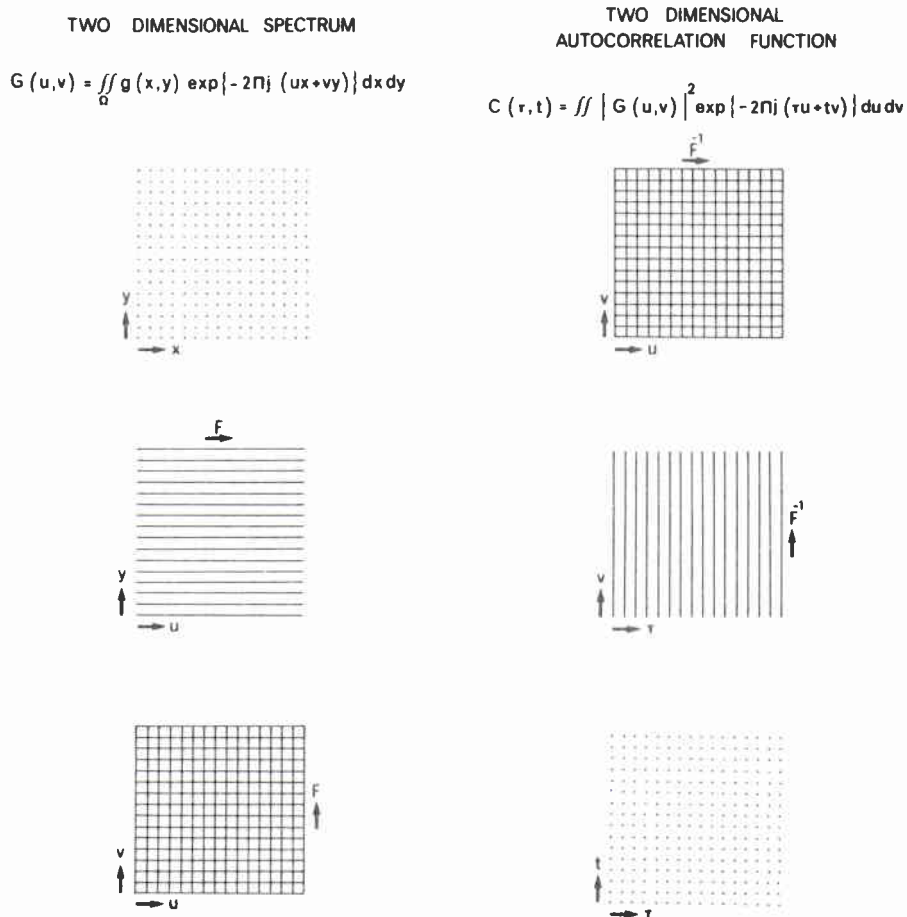


**Figure 2.** The method of computation (after Akal and Hovem 1978).

and accurate analog-to-digital conversion of a given contoured chart. This phase of work has been done by two separate operations: (1) Digitizing the contoured level using an electro-mechanical digitizer, which gives the coordinates of the contour lines in computer-compatible (UNIVAC 1106) format. (2) Construction of a matrix. For spectral analysis, numerical samples have to be obtained from a certain equally-spaced grid covering the contoured chart to be treated. This has been done by interpolating contoured values onto a rectangular grid by applying Laplacian or spline interpolation techniques. The type of interpolation is decided according to the

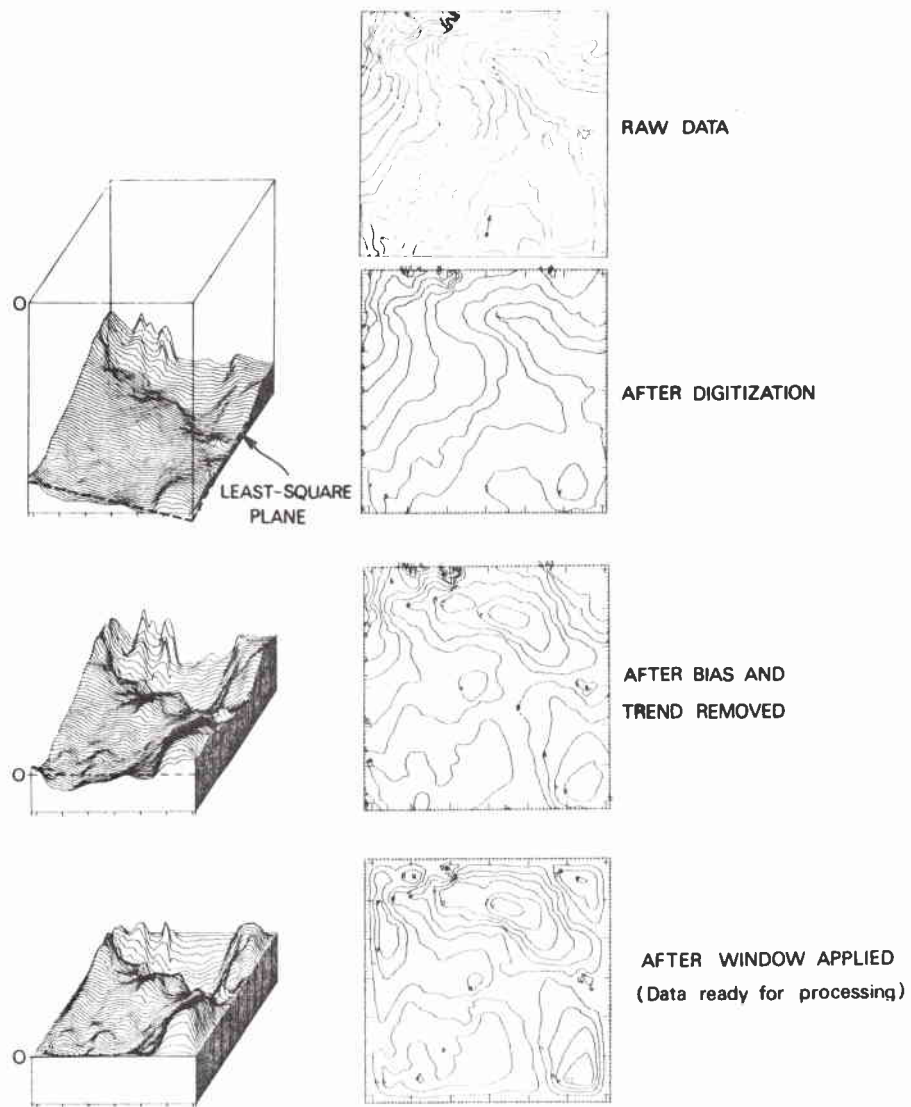


**Figure 3.** Preprocessing procedures (after Akal and Hovem 1978).

similarity obtained between analog and digitized data. Also, the grid size has to be carefully chosen to consider aliasing errors and available computer memory.

2. Removal of bias and trend from the data. The data we are dealing with are generally measured relative to a reference level. This means

that the surfaces we are interested in are superimposed on a rectangular box. For spectral analysis, it is desirable to transform the data to a zero mean value. After this, depending on the shape of the surface, a special correction may be needed to remove any wavelength longer than the surface being treated. This has been done by fitting a least-squares plane to the data for the two-dimensional detrending operation.

3. **Windowing and filtering.** To minimize the spectral distortion, there must be a broad and smooth data window without any sharp corners at the edges. Because of the size of the photographed area, the use of limited record size is inevitable in the two-dimensional spectral analysis, and truncation at the edges of a data window will erroneously introduce side lobes into the spectral domain. A two-dimensional filter that tapers off gradually with a cosine function towards both ends of the data window has been applied to suppress this effect. This certainly diminishes the effective area, but at the same time avoids severe distortion of the resulting spectral domains.

## DISCUSSION OF RESULTS

### Testing the Method

To facilitate understanding of the results obtained with this method, a simple test surface has been used. Figure 4 represents part of a cosinusoidal test surface  $g(x,y) = \cos [2\pi(x \cos \theta + y \sin \theta)]$  in  $30^\circ$  orientation ( $\theta = 30^\circ$ ).

After this test surface has been analyzed by this technique, its resulting power spectrum and autocorrelation functions are as shown in Figure 4. As expected, the orientation and wavelength content in the  $x,y =$  plane are converged by the impulse pair that constitutes the two-dimensional power spectrum of the test surface.

### Examples from Bottom Photographs

Five surfaces obtained from stereo seafloor photographs have been treated by this technique. These surfaces and the resulting power spectra and autocorrelation functions are shown in Figures 5, 6, 7, 8, and 9.

The surfaces in Figures 5 and 6 are taken from stereo photographs 12 m apart. Although these surfaces look completely different, as can be seen on

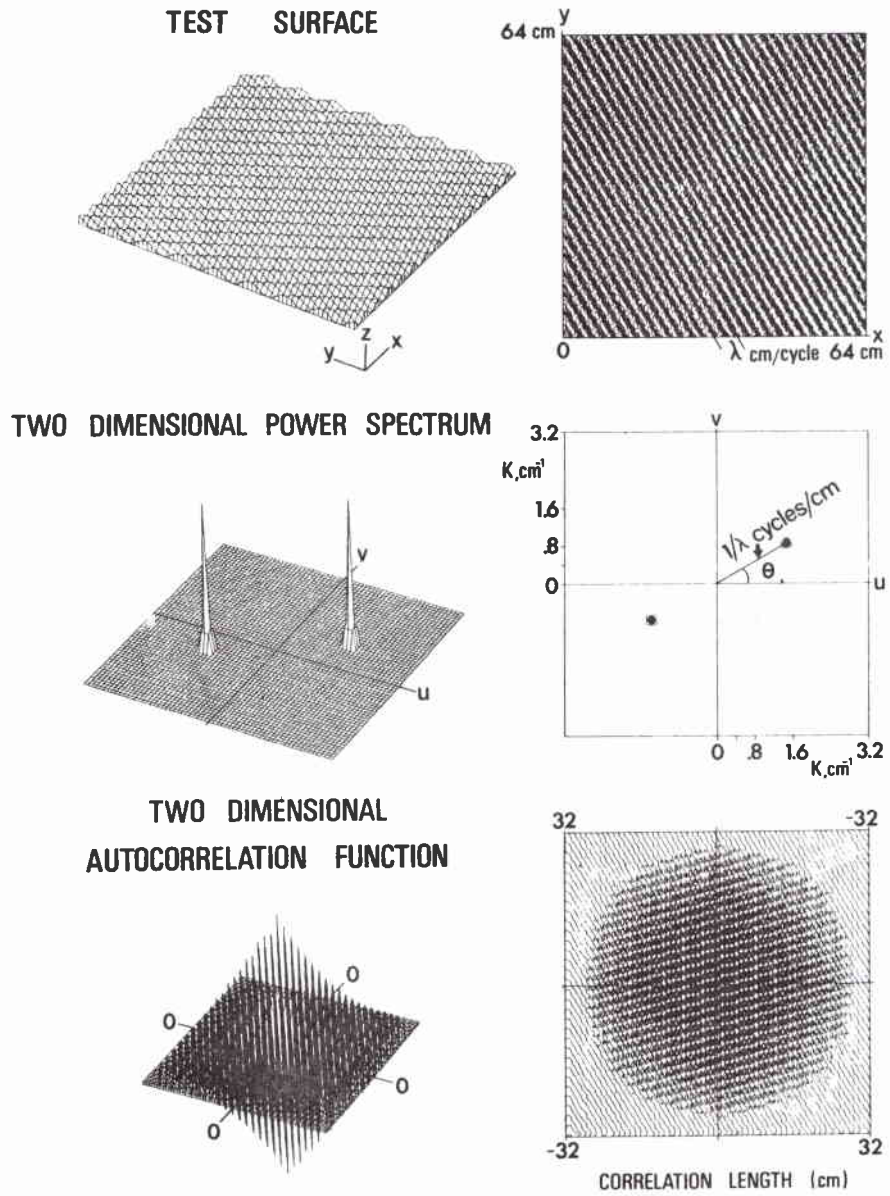


**Figure 4.** A cosinusoidal test surface,  
 $g(x,y) = \cos [2(x \cos \theta + y \sin \theta)]$ ,  $\theta = 30^\circ$   
 its two-dimensional power spectrum, and autocorrelation function (after Akal and Hovem 1978).



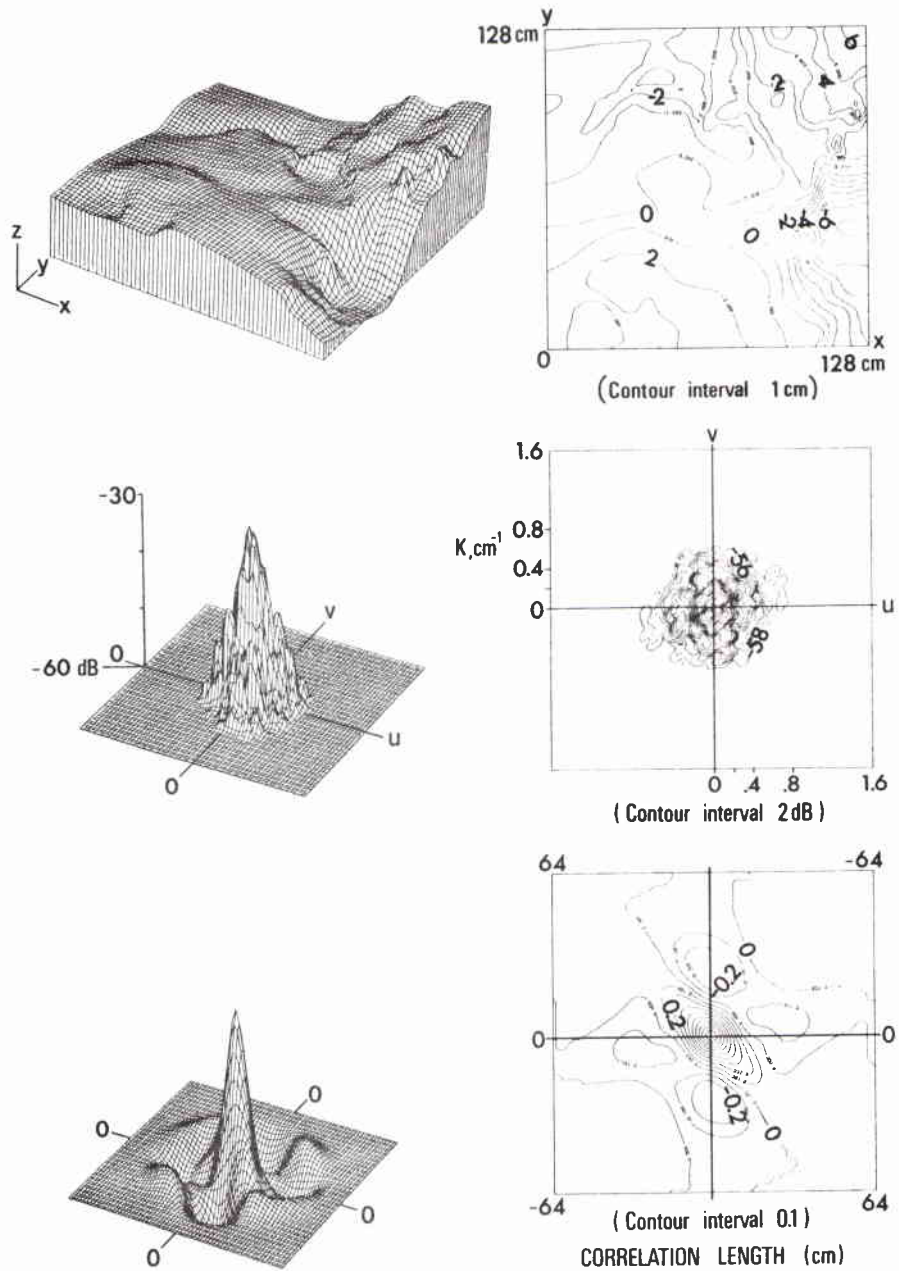


**Figure 6.** Another surface from bottom stereophotographs obtained 12 m away from the one shown in Figure 5, and the results obtained after processing.

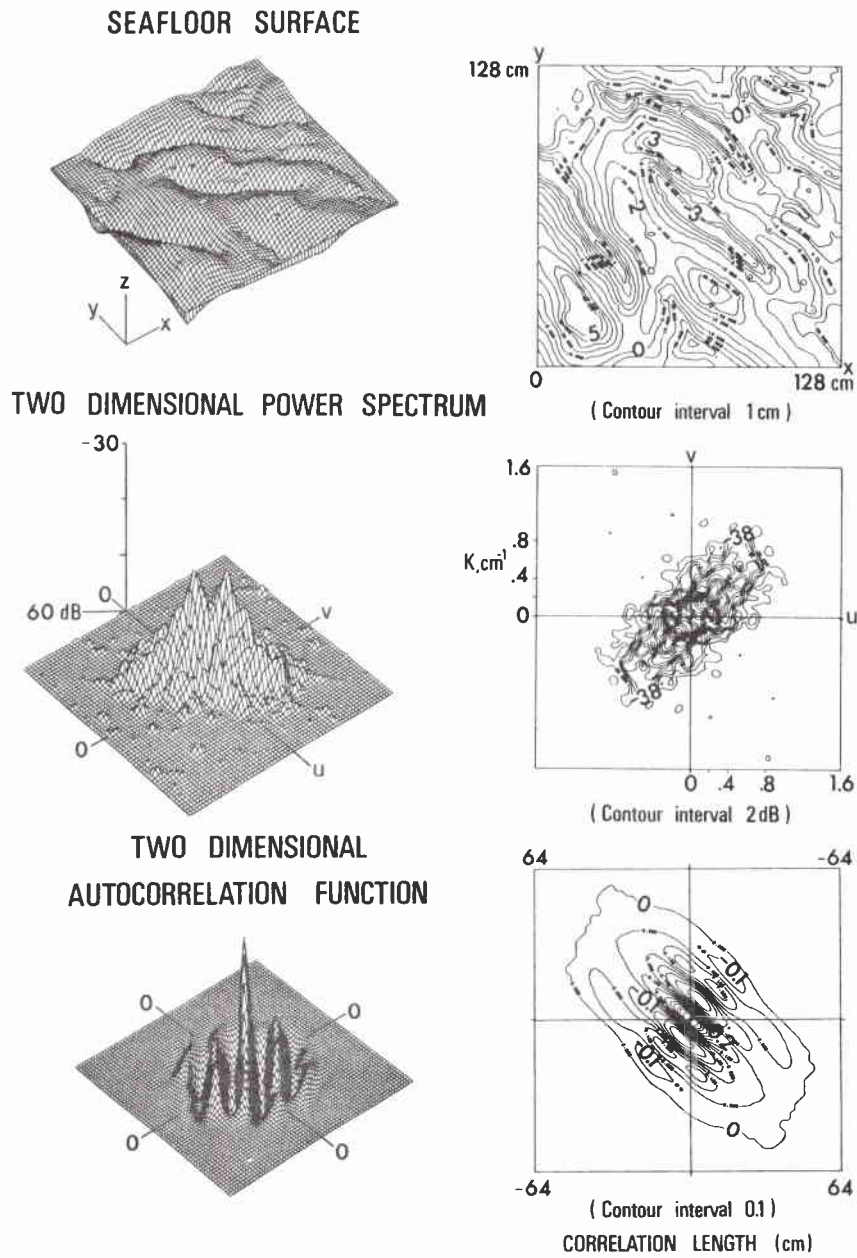


**Figure 7.** Seafloor with sand waves and the results obtained after processing.

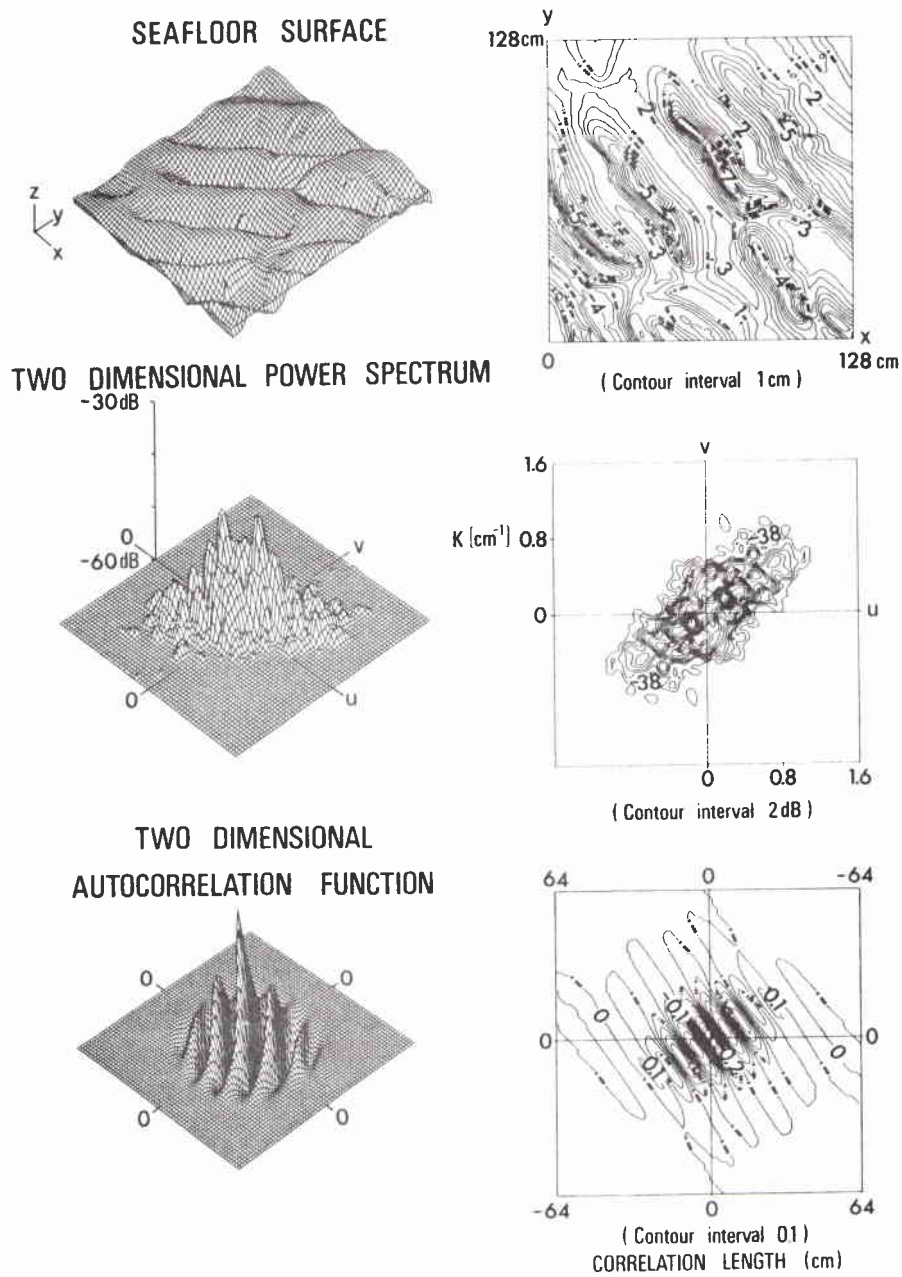


**Figure 8.** Another surface from the same area and the results obtained after processing.

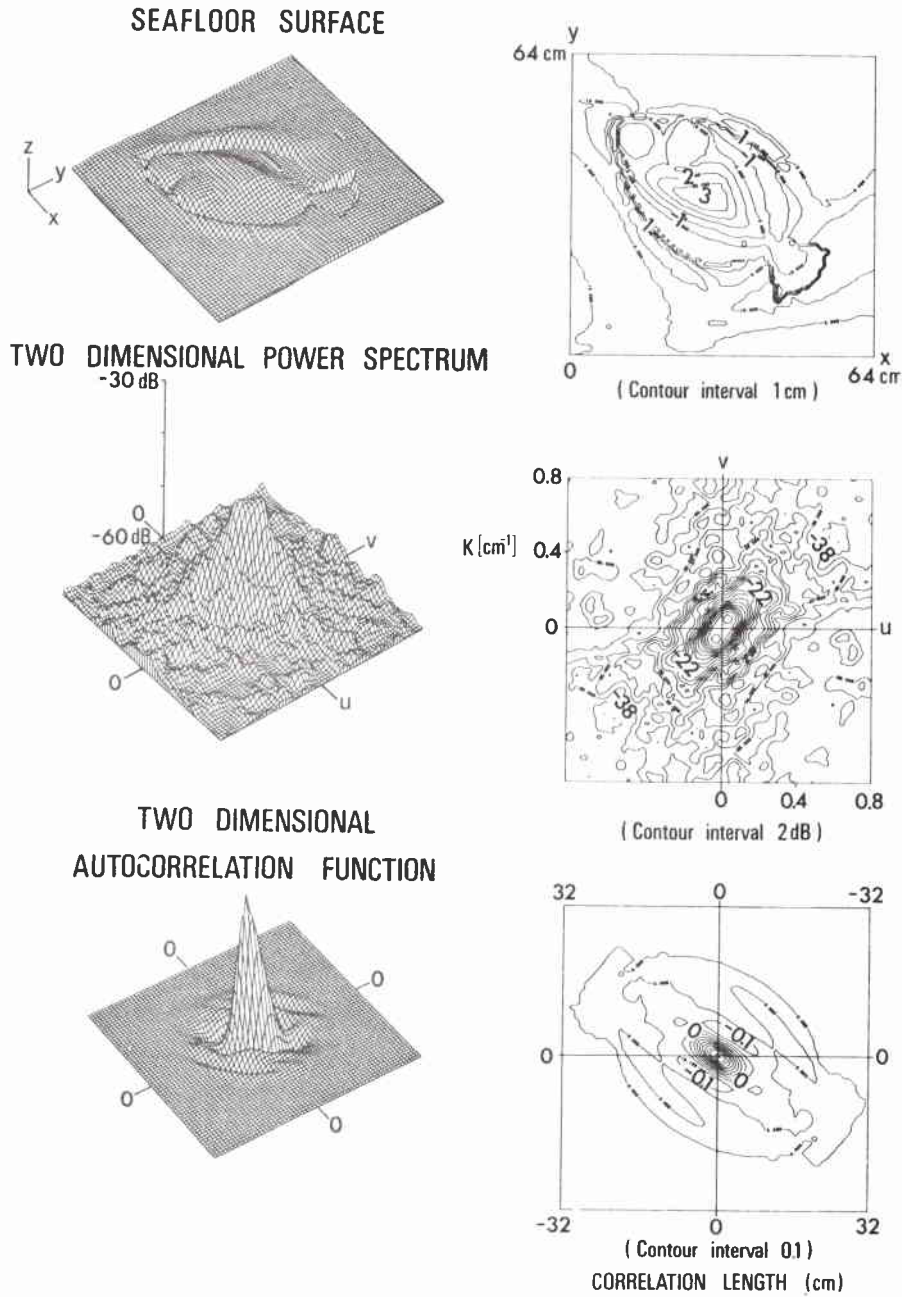


**Figure 9.** A plaiice buried in the sediments, together with its power spectrum and autocorrelation function.

power spectrum plots, the wavelength components of the bottom roughness are the same, except that there is a small directional change in orientation that appears more clearly on autocorrelation plots.

Figures 7 and 8 represent two parts of the seafloor with approximately a one-mile separation. The spectrum plots show two peaks corresponding to the wavelength content of the sand waves that are present in the area. Figure 9 shows a fish (plaice) buried in the sediments, together with its power spectrum and autocorrelation function. As expected, due to its form it gives much broader wavelength content.

## CONCLUSIONS

Using this method, the roughness of a contoured surface obtained from stereo photographs can be quantitatively described by its wave number composition and the direction of the roughness. This information is used for:

1. Investigation of the character, magnitude, and distribution of bottom roughness.
2. Classification of the quantitative roughness characteristics of the seafloor for different physiographic regions.
3. An input to different acoustic scattering and propagation models.

## ACKNOWLEDGMENTS

We wish to thank the Istituto Geografico Militare, Firenze (Italian Military Geographic Institute), and Mr. B. Turgutcan for the stereophotogrammetric graphic results they obtained from seafloor stereophotographs, and Mr. P. Nesfield for his support during computer program development.

## REFERENCES

- Akal, T., 1984. Acoustic characteristics of the sea floor: Experimental techniques and some samples from the Mediterranean Sea. In *Physics of Sound in Marine Sediments*, ed. L. Hampton, 447-480. New York; Plenum.
- Akal, T. and J. Hovem. 1978. Two-dimensional space-series analysis for sea floor roughness. *Marine Geotechnology* 3(2):171-182.

## APPENDIX:TWO-DIMENSIONAL POWER SPECTRAL DENSITY AND AUTO CORRELATION FUNCTIONS

Let us consider a two-dimensional function  $g(x,y)_\Omega$  representing a part of the seafloor surface in a rectangle of the  $x,y$ -plane (Figure 2). The Fourier transform is defined by

$$G(u,v) = \iint_{\Omega} g(x,y) \exp \{ -2\pi j(ux + vy) \} dx dy \quad (1)$$

where

$$g(x,y) = \iint G(u,v) \exp \{ 2\pi j(ux + vy) \} du dv \quad (2)$$

The squared amplitude spectrum  $|G(u,v)|^2$  is related to the two-dimensional correlation function  $C(r,t)$  by

$$C(r,t) = \iint |G(u,v)|^2 \exp \{ -2\pi j(ru + tv) \} du dv \quad (3)$$

or by making use of Equation (1):

$$C(r,t) = \iint g(x,y) g(x+r, y+t) dx dy \quad (4)$$

In the discrete case in which the function  $g(x,y)$  is sampled at regular intervals, the functions become slightly modified. Assume that the function  $g(x,y)$  is sampled at intervals  $\Delta x$  and  $\Delta y$  so as to produce a matrix

$$\begin{aligned} g_{k,i} &= g(k\Delta x, i\Delta y) \\ k &= 0,1,\dots,N-1 \\ i &= 0,1,\dots,M-1 \end{aligned} \quad (5)$$

The discrete Fourier transform evaluated at frequencies

$$u = r/N\Delta x \quad \text{and} \quad v = s/M\Delta y$$

is then

$$G(r/N\Delta x, s/M\Delta y) = G_{r,s} = \sum_{k=0}^{N-1} \sum_{i=0}^{M-1} \quad (6)$$

$$g_{k,i} \exp \{ -2\pi j(Kr/N + is/M) \}$$

KEYWORDS

AUTOCORRELATION FUNCTIONS  
BOTTOM ROUGHNESS  
FINE-SCALE ROUGHNESS  
PHOTOGRAMMETRY  
POWER SPECTRAL DENSITY  
PROPAGATION  
SCATTERING  
SMALL SCALE ROUGHNESS  
STEREO CAMERA  
UNDERWATER PHOTOGRAPHY

Using the Fast Fourier Transform (FFT) method for evaluation of  $G_{r,s}$  requires normally that both  $N$  and  $M$  be powers of two, and then  $G_{r,s}$  becomes evaluated for arguments  $r = 0, 1, \dots, N-1$  and  $s = 0, 1, \dots, M-1$ .

The discrete correlation function evaluated at points  $r = p\Delta x$  and  $t = q\Delta y$  is

$$C(p\Delta x, q\Delta y) = \sum_{k=0}^{N-1-p} \sum_{i=0}^{M-1-q} g_{k,i} g_{k+p,i+q} \quad (7)$$

In principle, this function can be computed directly following Equation (7), but to save time it is often preferable to compute it by using the FFT, that is:

$$C_{p,q} = \sum_{r=0}^{N-1} \sum_{s=0}^{M-1} G_{r,s}^2 \exp \{ -2\pi j (rp/N + sq/M) \} \quad (8)$$

The block diagram in Figure 2 illustrates the method of computation, which is in steps: first the  $x$  dependencies are transformed for each  $y$ , and then the  $y$  dependency is transformed.

SACLANTCEN SR-87

INITIAL DISTRIBUTION

	Copies		Copies
<u>MINISTRIES OF DEFENCE</u>		<u>SCNR FOR SAACLANTCEN</u>	
JSPHQ Belgium	2	SCNR Belgium	1
DND Canada	10	SCNR Canada	1
CHOD Denmark	8	SCNR Denmark	1
MOD France	8	SCNR Germany	1
MOD Germany	15	SCNR Greece	1
MOD Greece	11	SCNR Italy	1
MOD Italy	10	SCNR Netherlands	1
MOD Netherlands	12	SCNR Norway	1
CHOD Norway	10	SCNR Portugal	1
MOD Portugal	2	SCNR Turkey	1
MOD Spain	2	SCNR U.K.	1
MOD Turkey	5	SCNR U.S.	2
MOD U.K.	20	SECGEN Rep. SCNR	1
SECDEF U.S.	68	NAMILCOM Rep. SCNR	1
<u>NATO AUTHORITIES</u>		<u>NATIONAL LIAISON OFFICERS</u>	
Defence Planning Committee	3	NLO Canada	1
NAMILCOM	2	NLO Denmark	1
SACLANT	10	NLO Germany	1
SACLANTREPEUR	1	NLO Italy	1
CINCWESTLANT/COMOCEANLANT	1	NLO U.K.	1
COMSTRIKFLTANT	1	NLO U.S.	1
COMIBERLANT	1		
CINCEASTLANT	1	<u>NLR TO SAACLANT</u>	
COMSUBACLANT	1	NLR Belgium	1
COMMAIREASTLANT	1	NLR Canada	1
SACEUR	2	NLR Denmark	1
CINCNORTH	1	NLR Germany	1
CINC SOUTH	1	NLR Greece	1
COMNAVSOUTH	1	NLR Italy	1
COMSTRIKFORSOUTH	1	NLR Netherlands	1
COMEDCENT	1	NLR Norway	1
COMMARAIMED	1	NLR Portugal	1
CINCHAN	3	NLR Turkey	1
		NLR UK	1
		NLR US	1
		Total initial distribution	249
		SAACLANTCEN Library	10
		Stock	21
		Total number of copies	280